DYNAMICAL BEHAVIOUR OF NONLINEAR STRUCTURES UNDER VARYING LOAD

B. Dyniewicz and C.I. Bajer

Institute of Fundamental Technological Research, Polish Academy of Sciences, Warsaw, Poland

e-mail: bdynie@ippt.pan.pl, cbajer@ippt.pan.pl

1. Introduction

The problem is demonstrated on the example of a system that includes the so-called 'Gao beam,' which is modelled by a nonlinear beam equation. This study is motivated, in part, by the previous works on railway systems, see, e.g., [1, 2]. First, the track was subjected to a set of massless forces applied with more or less complex oscillators. Moreover, the dynamic properties and responses were not influenced by the additional inertia of the wheel-sets, which are invariably present in transportation applications. Indeed, their mass is about 750 kg per wheel and, thus, cannot be neglected. Second, the axial forces in rails were too simple. Moreover, the temperature of the rails can vary by more than 40 °C during a day and more than 70 °C during a year. Such variations in the temperature cause significant changes in the stresses and the mathematical models for the structures must take these processes into account. Here, we address the first item, while the issue of inclusion of thermal effects will be studies in the future. Such problems are of fundamental interest in railway transportation Models for a Gao beam were derived and simulated in [3], see also the references therein. They were investigated mathematically and computationally in [4].

2. Formulation and solution

We describe a model for the motion of a point-mass on a rail that is assumed to be a Gao beam, which has been constructed in [5]

$$(1) \qquad \rho w_{tt} + k w_{xxxx} + \gamma w_{txxxx} + (\overline{\nu} p - a w_x^2) w_{xx} = \rho f,$$

where here and below, the subscripts x and t denote partial derivatives, f is the density of applied distributed force (per unit mass), ρ is the material density (mass per unit cross-sectional area), $k = 2h^3 E_Y / 3(1 - \tilde{\nu}^2)$, $\overline{\nu} = (1 + \tilde{\nu})$, and $a = 3h E_Y$; $\tilde{\nu}$ and E_Y are the Poisson ratio and the Young modulus, respectively. Also, for mathematical reasons, we added a viscosity term γw_{txxxx}, with viscosity coefficient $\gamma > 0$, assumed to be small. We consider the moving mass m and the external force $f = f(x, t)$ subjecting a beam, with the traction $p = p(t)$ and the point load $P = P(t)$. The mass position is $\xi = \xi(t)$ the velocity $v = v(t)$, and the initial data w_0 and v_0; find the displacement field $w = w(x, t)$ for $x \in (0, 1)$ and $t \in [0, T]$, such that

$$(2) \qquad \rho w_{tt} + \delta(x - \xi) m w_{tt}(\xi, t) + k w_{xxxx} + \gamma w_{txxxx} - (a w_x^2 - \overline{\nu} p) w_{xx} = \rho f + \delta(x - \xi) P,$$
$$w(0, t) = w_x(0, t) = 0, \quad w(L, t) = w_x(L, t) = 0, \quad w(x, 0) = w_0(x), \quad w_t(x, 0) = v_0(x).$$

3. Results

Let us compare the load trajectory in the case of increasing p factor (Figure 1). First we assume low values of p to keep the structure in the bending range with a relatively low contribution of string vibration. We expect gradual change of traces during the first passage and we look for a significant change in successive passages. The first diagram (Figure 1a) depicts curves for p upto 1.0, while the second one exhibit traces for p upto 100.0. We notice that for low ranges of p the bending is the main phenomenon that occurs. For higher ranges the wave phenomenon that appear in a string or in an axially loaded bar dominates. At moderate p the process starts to elevate the follower point. This fact is visualized better in Figure 2. The second passage gives more
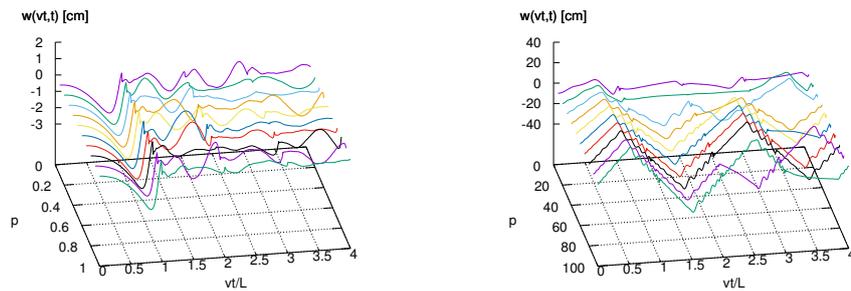
Figure 1: Load trajectories for various ranges of p.
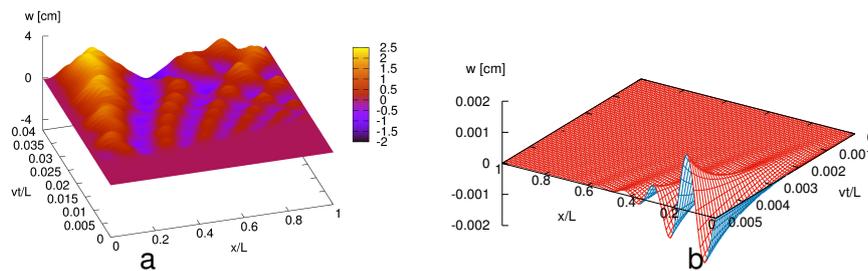
Figure 2: Displacement w in time (a) and displacement $w(x)$ at first steps of the process (b) (p=85).

flat surface in the diagram. Figure 2a shows the first stage of the passage through the span by the first load. The wave propagation from the loaded point is visible. At the beginning the beam is waved according to spatial parabolic terms of the differential equation. Wave effects are visible as well, especially as a reflection of waves from the end $x=L$. In such a case presence of the nonlinear Gao term strongly influences the response. The next Figure 2b is more contributing for better understanding the process. It shows the very early stage of the passage through the span by the first load. The lifted part of the beam at x/L=0.45 and 0.55 is noticeable. Wave crests have higher amplitudes than troughs. Moreover, careful sight at the beam axis at vt/L=0.0005 allows to notice small positive deflection of the segment 0.6<x/L<1.

4. Conclusions

The numerical simulations indicate that choosing the rail to be described by the Gao beam may be a better description if one is interested in the rail oscillations. First, for beams with a low bending stiffness the Gao beam is much more rigid than the Bernoulli-Euler beam. Second, a soft Bernoulli-Euler beam is characteristic of lower eigenfrequency than a rigid one. In the case of the Gao beam this relation is reversed. Third, higher external load increases the Gao beam features and strongly influences the frequency of the dynamic response.

References

[1] T. Dahlberg. Track issues. In Simon Iwnicki, editor, *Handbook of Railway Vehicle Dynamics*, pages 143–180. CRC Press, 2006.

[2] C. I. Bajer and R. Bogacz. Propagation of perturbances generated in classic track, and track with Y-type sleepers. *Arch. Appl. Mech.*, 74:754–761, 2005.

[3] D.Y. Gao. Finite deformation beam models and triality theory in dynamical post-buckling analysis. *Intl. J. Non-Linear Mechanics*, 35:103–131, 2000.

[4] K.T. Andrews, M.F. M'Bengue, and M. Shillor. Vibrations of a nonlinear dynamic beam between two stops. *Discrete and Continuous Dynamical System (DCDS-B)*, 12(1):23–38, 2009.

[5] C.I. Bajer, B. Dyniewicz, and M. Shillor. A gao beam subjected to a moving inertial point load. *Mathematics and Mechanics of Solids*, 23(3):461–472, 2018. DOI: 10.1177/1081286517718229.